Biophysical Chemistry 151 (2010) 81–85

Contents lists available at ScienceDirect

Biophysical Chemistry

journal homepage: http://www.elsevier.com/locate/biophyschem

DNA induced dimerization of a sulfhydryl surfactant in transfection agents studied by ESR spectroscopy

Laura Ciani [a], Gabriele Candiani [b], Alessia Frati [a], Sandra Ristori [a,*]

[a] Department of Chemistry and CSGI, University of Florence, Via della Lastruccia 3, 50019 Sesto F.no, Italy
[b] Department of Chemistry, Materials and Chemical Engineering "Giulio Natta", Politecnico di Milano, Via Mancinelli 7, 20131 Milano, Italy

ARTICLE INFO

Article history:
Received 13 April 2010
Received in revised form 4 May 2010
Accepted 19 May 2010
Available online 25 May 2010

Keywords:
DNA transfection
Electron Spin Resonance
Lipoplexes
Triazine surfactants
Disulfide bond

ABSTRACT

Synthetic vectors for gene delivery offer a wide variety of functional derivatization, which can be exploited to increase targeting and transfection efficacy. In this field, redox-sensitive agents based on the thiol/disulfide (–SH/–SS–) equilibrium are a class of promising transfectants.
Here the thiol group content in lipoplexes formed by a triazine-based sulfhydryl surfactant (SH14) and a plasmid (pGEFP-N1) was probed by Electron Spin Resonance (ESR) of appropriately tailored nitroxides. By modelling the time decay of ESR intensity, details on the process of lipoplex formation were obtained. It was found that the concentration of available –SH groups depended on the contact time between SH14 and DNA, suggesting that lipoplex formation entailed disulfide bridge formation among SH14 molecules.
This finding represents the first experimental evidence that the –SH/–SS– equilibrium plays a role in lipoplex formation when DNA is complexed by sulfhydryl-based transfecting agents, which may have profound influence on their mechanism of action.

1. Introduction

Gene therapy involves the introduction of a missing gene into the cell nucleus followed by the expression of genetic information (transfection). The use of amphiphilic aggregates built with cationic lipids is currently investigated in the form of complexes with DNA (*lipoplexes*) [1–5]. Till now, the main problem encountered in using lipoplexes for transfection experiments is scarce efficacy in DNA release to cell cytoplasm. This is believed to be the most impeding factor to cause the generally poor efficacy of cationic non-viral vectors, though their use is a therapeutically attractive option. Synthetic vectors are readily available (several transfection reagents are commercial products), versatile, and scarcely toxic.

In recent years, surfactants bearing the sulfhydryl moiety have been suggested as non-viral carriers for gene therapy [6–8]. In particular, triazine cationic surfactants have been synthesized and tailored with the aim of preparing lipid systems with improved transfection properties, i.e. dimerizable redox-sensitive thiol groups [9]. These triazine-based surfactants have shown low cytotoxicity and high transfection efficacy on a variety of eukaryotic cells [6,7]. The transfection mechanism is supposed to rely on the oxidation of –SH in the triazine monomer to –SS– in the corresponding dimer, which affects lipoplex stability. This hypothesis has been formulated to account for the observed results and by comparison with similar molecules [10–13]. However, a direct evidence of dimer formation is still lacking.

Electron Spin Resonance (ESR) Spectroscopy of nitroxides (NTXs) is widely used to obtain clues on biological problems involving electron transfer. The metabolic fate of stable NTXs in living systems is prevalently determined by reduction to the corresponding diamagnetic hydroxylamine [14–16]:

$$>NO + e^- + H^+ \rightarrow >N{-}OH \quad (1)$$

with resultant decrease of the spectral ESR intensity as a function of time. This has been found in many cases, from isolated cell components to tissues [17–20].

Reaction (1) is particularly informative when the reducing agent is the –SH group. The equilibrium –SH/–SS– is an important parameter in many biological processes such as cell signalling and enzyme action, as it happens, for instance, for the reduced glutathione/glutathione disulfide couple (GSH/GSSG), which is involved in oxidative stress and free radical pathologies [21–23], in folding of secreted proteins [24] and intracellular delivery of drugs and genetic material [25,26]. Togasahi et al. [27,28] have used the ESR spectra of Proxyl-carbamoyl NTX as a probe for monitoring the availability of GSH in living mice and have shown that the starting unreduced radicals can be recovered in some circumstances.

Tang and Hughes [29,30] have used the disulfide bond as bridge functionality in cationic transfection lipids. These authors suggest that reduction of the disulfide linker by the intracellular GSH ensures the collapse of the DNA/lipid complex. ESR has also shown to be a powerful means to determine the kinetics of –SH redox reactions. To this aim Khramtsov et al. [31,32] employed unusual disulfide

* Corresponding author. Tel.: +39 0554573048; fax: +39 0554573036.
E-mail address: ristori@csgi.unifi.it (S. Ristori).

0301-4622/$ – see front matter © 2010 Elsevier B.V. All rights reserved.
doi:10.1016/j.bpc.2010.05.010

nitroxide biradicals (DNB), while more standard NTXs were used in other systems [33–35].

In this paper a plasmid encoding for the Enhanced Green Fluorescent Protein (pEGFP-N1) was used as genetic material to be complexed in lipoplexes by a triazine surfactant (SH14). The oxidation of SH14 in free and plasmid-loaded aggregates was monitored by ESR of two amphiphilic NTXs (5DSA, and CAT12) and one water-soluble NTX (Proxyl-carboxylate), which were used as scavenger of available –SH groups. ESR thus allowed to obtain the first experimental evidence of –SH oxydation in transfection systems.

2. Experimental section

Triazine-based SH14 (2-[4-(3-aminopropylamine)-6(tetradecylamino)-1,3,5-triazine-2-ylamino]-ethanthiol-bis-trifluoroacetate) is shown in Fig. 1. The polar head is based on the 1,3,5-triazine core. The three amine bridges render the molecule stable in a water environment. The synthesis of SH14 is described in ref. [6].

SH14 and its water solutions were maintained at –20 °C and 4 °C, respectively. The oxidized R–SS–R (SS14) was obtained through a four step procedure from 1,3,5-trichloro-2,4,6-triazine [6].

The critical micelle concentrations (cmc) of SH14 was evaluated by conductimetry (Coulter Delsa 440SX), recording the specific conductivity of SH14 water solutions in the range 10^{-2}–10^{-4} mol/L. The obtained values were fitted by two straight lines and the intersection point, which is due to micelle formation, was found at 1.5×10^{-3} mol/L.

Plasmid DNA (4.7 kb) encoding for Enhanced Green Fluorescent Protein (pEGFP-N1) under the control of the human cytomegalovirus (CMV) promoter was purchased from Clontech Laboratories (Paris, France).

5-Doxyl-stearic acid spin probes (5DSA), 4-(dodecyl-dimethylammonium) 2,2,6,6-tetramethylpiperidine 1-oxyl bromide (CAT12) were purchased from Sigma Chemicals (Munchen, Germany) and 2,2,5,5-tetramethylpyrrolidinyloxy-3-carboxylate sodium salt, (Proxyl-carboxylate) was obtained from Molecular Probe (Eugen, Oregon). All NTXs were used as received.

Stock ethanol solutions of 5DSA, CAT12 (10^{-3} mol/L) and Proxyl-carboxylate (10^{-4} mol/L) probes were prepared. Each spin probe solution was evaporated in a vial prior to SH14 or lipoplex addition. The added NTX concentration was kept constant at 5×10^{-5} mol/L, since this value was the best compromise between signal intensity and the requirement for any probe of not inducing alteration in the investigated system. Conductivity and ESR measurements were used for double check these effects.

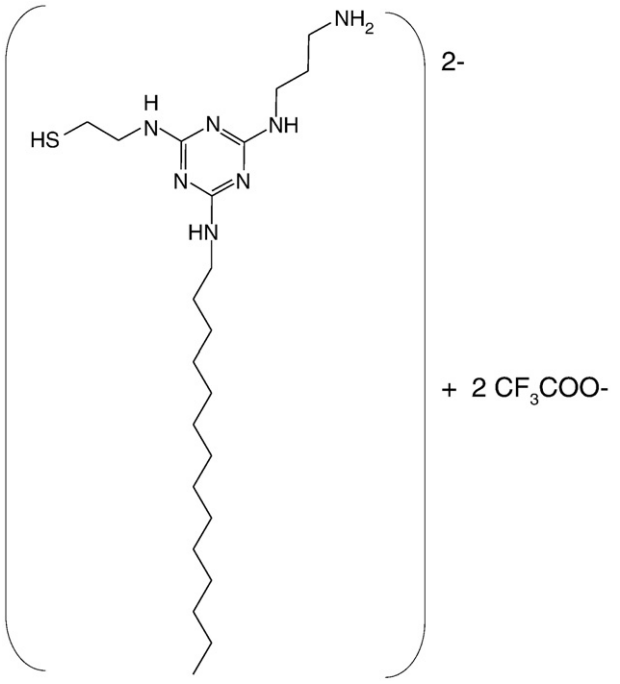

Fig. 1. Structure of the SH-14 (2-[4-(3-aminopropylamine)-6(tetradecylamino)-1,3,5-triazine-2-ylamino]-ethanthiol-bis-trifluoroacetate).

All samples were equilibrated with spin probes for 15 min at room temperature, to ensure complete uptake of the NTXs into aggregates, and then transferred in a glass capillary for ESR runs (25 °C).

Complexes with pEGFP-N1 were obtained by adding the plasmid to SH14 micelles at the desired charge ratio (CR = +/−). CR was calculated as the number of positive charges due to the polar head of SH14 divided by the negative charges on DNA phosphates. Based on previous *in vitro* experiments [7] we chose to work at fixed CR 10. This value corresponds to the most effective ratio for transfection. Lipoplex samples were left to equilibrate at room temperature for different times (from 15 min to 48 h), before adding the spin probe. These time intervals, required for SH14/pEGFP-N1 complex formation, will be henceforth referred to as compaction times.

ESR spectra were recorded in the continuous wave mode with a Bruker ESR spectrometer model 200D, operating at X-band (9.5 GHz). Data acquisition and handling were carried out with the ESR software commercialised by STELAR (Meda, Italy). The temperature was controlled with Bruker VT 3000 apparatus (accuracy ± 0.2 °C).

Kinetic data were obtained from the time variation of the second line intensity in the ESR triplet of NTXs for each decay series. This procedure was based on the experimental evidence that the line shape of all recorded ESR spectra did not change either with time or as a result of spin–spin broadening mechanisms. Signal height decrease was therefore entirely attributed to the reduction of NTXs to the corresponding diamagnetic hydroxylamines.

3. Results and discussion

Typically, the ESR spectrum of a simple NTX in rapid motion is composed of three adsorption lines due to the hyperfine coupling of the unpaired electron with the ^{14}N nucleus ($I_N = 1$). The line shape depends on the properties of the environment sensed by the >NO group, such as molecular ordering and/or motional restriction. Fig. 2 compares the ESR spectra of three NTXs used in this work, interacting either with SH14 micelles or with CR 10 lipoplexes.

The 5DSA spectrum in SH14 micelle solution was characteristic of slow moving radicals (Fig. 2A, black line). This behaviour is widely documented in the literature for complex amphiphilic systems and was attributed to the presence of aggregates, incorporating the probe because of its hydrocarbon chain. The motion of 5DSA was further slowed down when pEGFP-N1 was added to the system (Fig. 2A, red line), as evidenced by the increase in separation between the first and third absorption ($2A'_{||}$). This meant that relatively strong electrostatic interactions between the phosphate groups of the nucleic acid and the positively charged triazine head induced rearrangement of SH14 aggregates. In the same conditions CAT12 and Proxyl-carboxylate maintained a fast tumbling spectrum (Fig. 2B and C, respectively); however, a small progressive motional restriction was evidenced in passing from pure water (supplementary information) to SH-14 micelles to lipoplex solution.

Our main interest in these systems was the signal decay due to NTX reduction and for this purpose CAT12 was our best choice. In fact, 5DSA gave very poor signal to noise ratio because the spectrum of the spin probe in slow motion is broad and it was difficult to measure the signal intensity at low concentration. Proxyl-carboxylate showed sharp transitions, which were ideal to follow low ESR intensities, but in this case the time required for NTX reduction (4–8 h) was long enough to allow the onset of side effects. Indeed, it has been reported [33] that if the reduction time of a NTX by –SH groups is long, attention should be put to oxidative effects by dissolved molecular

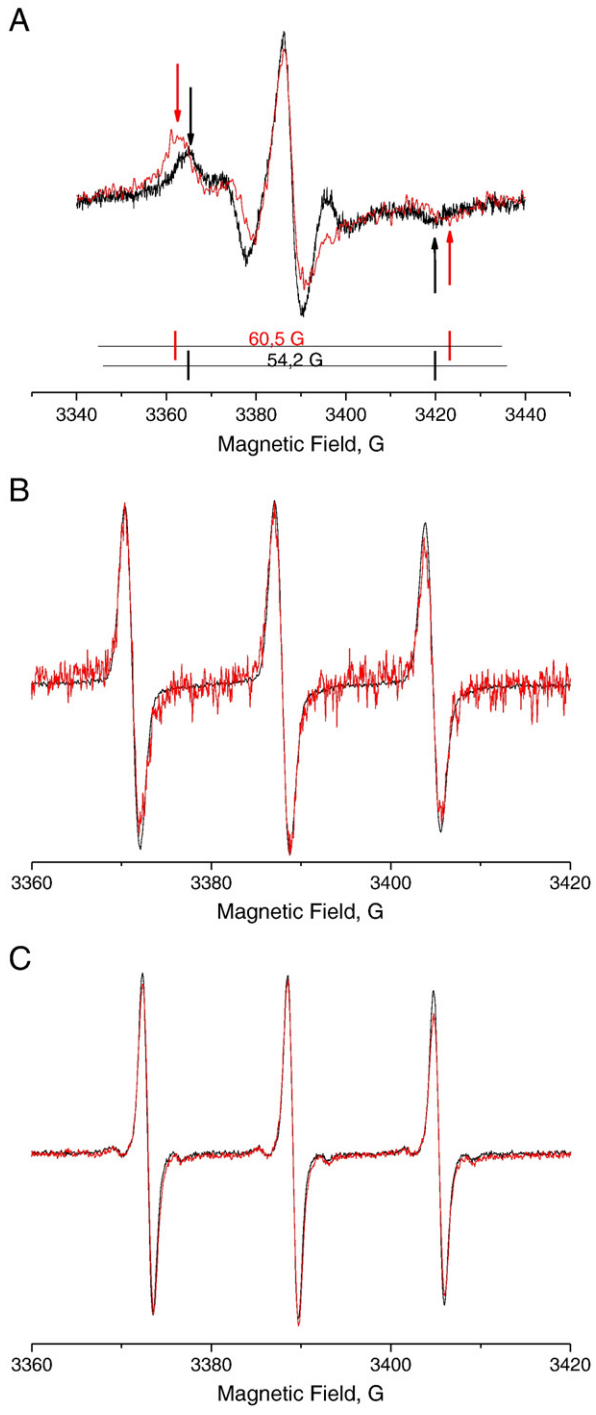

Fig. 2. Panel A: 5DSA; panel B: CAT12; panel C: Proxyl-carboxylate. ESR spectra of 5×10^{-5} mol/L NTX inserted into 5×10^{-3} mol/L SH14 micelles (black lines) and into CR 10 lipoplexes prepared with the same SH14 concentration (red lines). Lipoplex formation, in this case, was allowed to proceed for 24 h before adding the spin probe (see text for further details).

oxygen, which diffuses slowly into the system and is able to reoxidize the hydroxylamine to the corresponding NTX. Therefore, CAT12 resulted a good trade off between intensity and a suitable time dependent NTX reduction.

We followed CAT12 ESR signal evolution and kinetic data were extracted from height variations in the second line of the NTX spectrum at fixed time intervals (2 min). As discussed above, the signal height decrement was attributed to nitroxide reduction, according to the following scheme:

$$2R{-}SH + 2{>}NO \rightarrow R{-}SS{-}R + 2{>}NH. \quad (2)$$

Fig. 3 shows the signal decay of CAT12 inserted in SH14 micelles and in SH14/pEGFP-N1 lipoplexes at CR 10. For comparison, the behaviour of CAT12 in the presence of dimerized SH14 counterpart (named SS14) at the same concentration of positive charges is also shown.

Good linearity of the intensity decay in a semilogarithmic plot ensured that a first order reaction of the type:

$$-d[NTX]/_d t = k_v[NTX] \quad (3)$$

governed the NTX reduction in the presence of SH14 micelles. The kinetics constant k_v was $5.7\times10^{-2}\ s^{-1}$.

The signal intensity was below ESR detection limit for ~1 day and after this time it slowly re-increased. This recovering was attributed to the oxidative effect of dissolved molecular oxygen, as previously observed in other cases [33]. We were not especially interested in the change occurring when oxygen concentration in the sample is of the order of magnitude of NTX. Therefore no thorough investigation was made on this point.

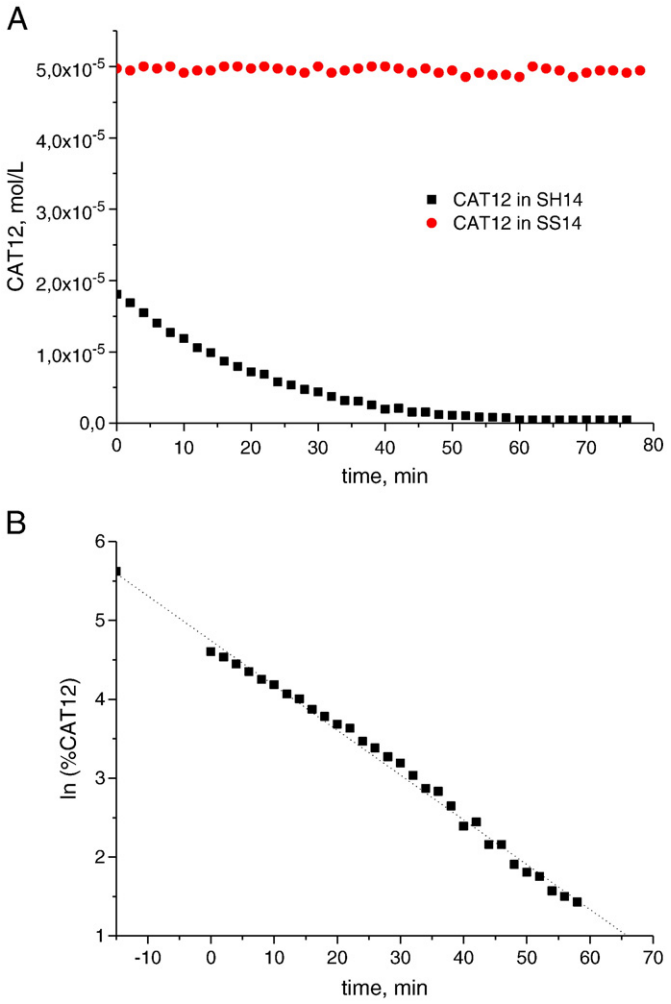

Fig. 3. Panel A: Time decay of CAT12 (5×10^{-5} mol/L) ESR intensity in SH14 micelles (5×10^{-3} mol/L) and in SS14 solution at the same charge concentration. Panel B: Semilogarithmic plot of CAT12 ESR intensity in SH14 micelles expressed as percentage of the initial concentration. The dotted line is the best fit performed with a first order kinetic model (Eq. (3) in the text).

Since samples were let to equilibrate with CAT12 for 15 min before starting ESR registration to ensure complete uptake of the spin probe, the first intensity value could not be attributed to 100% CAT12 concentration. To obtain this value the linear fitting was extrapolated up to $t=-15$ min, while $t=0$ was the first recorded CAT12 intensity.

Similar effects were observed when pEGFP-N1 was incorporated into the system. Fig. 4 shows the ESR signal decrease in the presence of nucleic acid at different compaction times for several representative systems. The same linear fitting procedure to obtain the CAT12 concentration at $t=0$ was used for these curves.

As shown in Fig. 4, the concentration of CAT12 at $t=0$ steadily increased at increasing compaction time. Considering that the starting value of NTX concentration was the same in all cases, it meant that at longer compaction time, fewer –SH groups were available for the redox process which generate the ESR silent hydroxylamine. To confirm this interpretation we observe that the time dependence of CAT12 intensity in the presence of preformed dimer SS14 (Fig. 3A, red diamonds) did not show any decay.

The lipoplexes equilibrated for 15 and 23 min gave very good linearity up to 60 min in a semilogarithmic scale. We could thus consider this reaction of pseudo-first order. In fact, the SH14 concentration was high enough to consider it constant in the following analysis:

$$[A] = \left[A_0 e^{-k' t}\right] \tag{4}$$

$$\ln[A] = \ln[A_0] - k' t \tag{5}$$

$$k' = k[B] \tag{6}$$

where $[A]$ is the concentration of CAT12 and $[B]$ the concentration of SH14.

It is to be noted that in the case of lipoplexes with 15 min compaction time k' was larger (i.e. the reduction of the NTX was more rapid) than k_v for SH14 micelles, suggesting that a different reaction mechanism was acting compared to micelles. We believe that in the case of micelles only the reduction of NTX took place (see Eq. (2)), while in presence of DNA the system was more complex and k' also depended on the SH14 initial concentration.

In lipoplexes equilibrated for longer compaction times, the linearity observed above did not occur and a second order mechanism had to be considered. Indeed, all decay curves of CAT12 equilibrated with lipoplex could be fitted by the following equations:

$$kt = \frac{1}{[B_0]-[A_0]} \ln\left(\frac{{}^{[B]}/_{[B_0]}}{{}^{[A]}/_{[A_0]}}\right) \tag{7}$$

$$A = A_0 - \frac{A_0 B_0\left(1-e^{(B_0-A_0)kt}\right)}{A_0 - B_0 e^{(B_0-A_0)kt}} \tag{8}$$

with kinetic constant $k=701.7$ M/s ($R^2=0.9972$). Table 1 reports the concentration of CAT12 and SH14 at $t=0$ obtained from the fitting.

The first two values in Table 1, calculated by second order fitting were in perfect agreement with those reported in Table 2 and calculated by pseudo-first order fitting.

Fig. 5 shows a comparison among residual CAT12 concentration during the ESR decay experiments.

The observed trend indicated that CAT12 residual concentration increased with increasing contact time during formation of CR 10 lipoplexes. This was correlated with decreasing SH14 monomer content, due to more extended dimer formation.

Table 1
Best fit values for different compaction times lipoplexes at CR 10, analyzed as second order kinetics.

Compaction time	CAT12 at $t=0$ (mol/L)	SH14 ± 2.5% (mol/L)
15 min	1.6×10^{-5}	1.1×10^{-4}
23 min	3.2×10^{-5}	4.2×10^{-5}
30 min	3.3×10^{-5}	4.4×10^{-5}
3 h	3.4×10^{-5}	4×10^{-5}
24 h	4×10^{-5}	1.7×10^{-5}
37 h	4.4×10^{-5}	1.4×10^{-5}
48 h	4.7×10^{-5}	8.3×10^{-6}

Table 2
Best fit values for CR 10 lipoplexes with compaction time of 15 and 23 min, analyzed as pseudo-first order decays.

Compaction time (min)	CAT12 at $t=0$ (mol/L)	k', s^{-1}
15	1.6×10^{-5}	7×10^{-2}
23	3.2×10^{-5}	3×10^{-2}

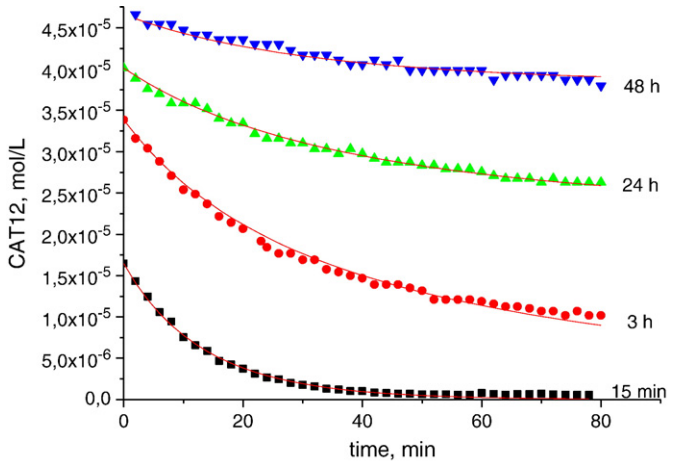

Fig. 4. ESR decay curves of CAT12 in the presence of CR 10 lipoplexes equilibrated with the same amount of NTX (5×10^{-5} mol/L at $t=-15$ min) and different compaction time.

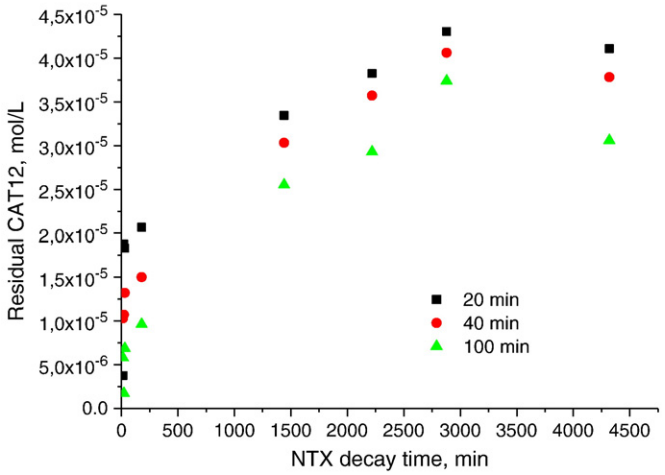

Fig. 5. CAT12 residual concentration in CR 10 lipoplexes at fixed values of NTX decay time. Black squares: compaction time 20 min; red diamonds: compaction time 40 min; green triangles: compaction time 100 min.

4. Conclusions

In this work we investigated the ESR behaviour of NTXs as scavenger for residual –SH groups in micelles and lipoplexes of triazine-based amphiphiles. The >NO group is able to induce –SS– bridging of thiols, in consequence of its reduction to the corresponding ESR silent hydroxylamine. We observed the same electronic transfer when CAT12 was added to SH14 micelles. In this case the redox process could be modelled as first order reaction. On the other hand, in the presence of SH14/pEGFP-N1 lipoplexes the system showed a more complex behaviour. In particular, we observed that longer compaction times decreased the amount of available SH groups. This proved that during compaction time SH14 dimerized to SS14, which was no longer able to reduce CAT12, thus confirming the hypothesis of Candiani et al. that DNA favours the formation of –SS– bridges in these transfection agents [7].

The ESR intensity decay in CR 10 lipoplexes was fitted as pseudo-first or second order kinetics. Such scheme is probably an approximation of the actual reaction taking place in these systems. Indeed, reaction (2) can be considered a real first order electron transfer, but in the case of lipoplexes, dimer formation due to the presence of pEGFP-N1 could also contribute to decreasing SH concentration. Therefore, the ESR intensity decay depended both on NTX and SH14 groups. Similar results were obtained in other complex systems, where different single step reactions concurrently take place [20,36] In these systems, the kinetics of the overall redox process also appeared as second order, but in depth analysis of the reaction mechanism showed that more than one first order electron transfer simultaneously occurred during NTX reduction [37,38].

Acknowledgements

The authors are indebted to the University of Florence, the Consorzio Interuniversitario per lo Sviluppo di Superfici e Grandi Interfasi (CSGI), and the Politecnico di Milano (Grant 5 per mille junior) for financial support. Prof G. Martini is acknowledged for interesting discussion during the preparation of this manuscript. Thanks are also due to KemoTech s.r.l. for providing SS14 and SS14 surfactants.

Appendix A. Supplementary data

Supplementary data associated with this article can be found, in the online version, at doi:10.1016/j.bpc.2010.05.010.

References

[1] C.R. Safinya, Structures of lipid–DNA complexes: supramolecular assembly and gene delivery, Curr. Opin. Struct. Biol. 11 (2001) 440–448.
[2] P.L. Felgner, T.R. Gadek, M. Holm, R. Roman, H.W. Chan, M. Wenz, J.P. Northrop, G.M. Ringold, N. Danielsen, Lipofection: a highly efficient, lipid-mediated DNA transfection procedure, Proc. Natl. Acad. Sci. U. S. A. 84 (1987) 7413–7417.
[3] S.A. Audouy, L.F.D. Leji, D. Hoekstra, G. Modena, In vivo characteristics of cationic liposomes as delivery therapy, Pharm. Res. 19 (2002) 1589–1605.
[4] A.D. Miller, Cationic liposomes for gene therapy, Angew. Chem. Intern. Ed. 37 (1998) 1768–1785.
[5] A. Salvati, L. Ciani, S. Ristori, G. Martini, A. Masi, A. Arcangeli, Physico-chemical characterization and transfection efficacy of cationic liposomes containing the pEGFP plasmid, Biophys. Chem. 121 (2006) 21–29.
[6] G. Candiani, M. Frigerio, F. Viani, C. Verdelli, C. Sala, L. Chiamenti, N. Zaffaroni, M. Folini, M. Sani, W. Panzeri, M. Zanda, Dimerizable redox-sensitive triazine-based cationic lipids for in vitro gene delivery, ChemMedChem 2 (2006) 292–296.
[7] G. Candiani, D. Pezzoli, M. Cabras, S. Ristori, C. Pellegrini, A. Kajaste-Rudnitski, E. Valenzi, C. Sala, M. Zanda, A dimerizable cationic lipid with potential for gene delivery, J. Gene Med. 10 (2008) 637–645.
[8] V.V. Kumar, A. Chaudhuri, On the disulfide-linker strategy for designing efficacious transfection lipids: an unexpected transfection profile, FEBS Lett. 571 (2004) 205–211.
[9] Surfactant triazine compounds and their use, USPatent no. 5240499, by R. Az, W. Schwab, D. Schnaitmann, 1993.
[10] E. Dauty, J.-S. Remy, T. Blessing, J.-P. Behr, Dimerizable cationic detergents with a low cmc condense plasmid DNA into nanometric particles and transfect cells in culture, J. Am. Chem. Soc. 123 (2001) 19227–93134.
[11] G. Zuber, L. Zammut-Italiano, E. Dauty, J.P. Behr, Targeted gene delivery to cancer cells: directed assembly of nanometric DNA particles coated with folic acid, Angew. Chem. 42 (2003) 2666–2669.
[12] C. Chittimalla, L. Zammut-Italiano, G. Zuber, J.P. Behr, Monomolecular DNA nanoparticles for intravenous delivery of genes, J. Am. Chem. Soc. 127 (2005) 11436–11441.
[13] V.V. Kumar, A. Chaudhuri, On the disulfide-linker strategy for designing efficacious cationic transfection lipids: an unexpected transfection profile, FEBS Lett. 571 (2004) 205–211.
[14] E.J. Rauckman, G.M. Rosen, L.K. Griffeth, Enzymatic reactions of spin labels, Spin Labeling in Pharmacology, Academic Press, New York, 1989, pp. 175–190.
[15] M. Sentjurc, Investigations of redox reactions in biological systems by EPR, Exp. Technol. Phys. (Berlin) 38 (1990) 269–276.
[16] S. Belkin, R.J. Melhorn, K. Hideg, O. Hankowsky, Reduction and destruction rates of nitroxide spin labels, Arch. Biochem. Biophys. 256 (1987) 232–243.
[17] M. Kveder, M. Sentjurc, M. Shara, Spin probe reduction in cells and tissues, Magn. Reson. Med. 8 (1988) 241–247.
[18] M. Kveder, A. Krisko, G. Pifat, H.J. Steinhoff, The study of structural accessibility of free thiol groups in human low-density lipoproteins, Biochim. Biophys. Acta 1631 (2003) 239–245.
[19] M. Schara, S. Pecar, J. Svetek, Reactivity of hydrophobic nitroxides in lipid bilayers, Colloids Surf. 45 (1990) 303–312.
[20] G.I. Roshchupkina, A.A. Bobko, A. Bratasz, V.A. Reznikov, P. Kuppusamy, V.A. Khramtsov, In vivo ESR measurement of glutathione in tumor-bearing mice using improved disulfide biradical probe, Free Radic. Biol. Med. 45 (2008) 312–320.
[21] P.S. Samiec, C. Drews-Botsch, E.W. Flagg, J.C. Kurtz, P. Sternberg Jr, R.L. Reed, D.P. Jones, Glutathione in human plasma: decline in association with aging, age-related molecular degeneration, and diabetes, Free Radic. Biol. Med. 24 (1998) 699–704.
[22] A.P. Arrigo Gene, Expression and the thiol redox state, Free Radic. Biol. Med. 27 (1999) 936–944.
[23] H. Sies, Glutathione and its role in cellular functions, Free Radic. Biol. Med. 27 (1999) 916–921.
[24] S. Gleiter, J.C.A. Bardwell, Disulfide bond isomerization in prokaryotes, Biochim. Biophys. Acta 1783 (2008) 530–534.
[25] A.N. Koo, H.J. Lee, S.E.K., J.H. Chang, C. Park, C. Kim, J.H. Park, S.C. Lee, Disulfide-cross-linked PEG-poly(amino acid)s copolymer micelles for glutathione-mediated intracellular drug delivery, Chem. Commun. (2008) 6570–6572.
[26] S.H. Kim, J.H. Jeong, S.H. Lee, S.W. Kim, T.G. Park, Local and systemic delivery of VEGF siRNA using polyelectrolyte complex micelles for effective treatment of cancer, J. Control. Release 129 (2008) 107–116.
[27] H. Togashi, T. Matsuo, H. Shinzawa, *In vivo* imaging of increased oxidative stress in the liver by the electron spin resonance-computed tomography, Res. Commun. Mol. Pathol. Pharmacol. 107 (2000) 197–217.
[28] H. Togashi, K. Oikawa, T. Adashi, K. Sugahara, J. Ito, T. Takeda, H. Watanabe, K. Saito, T. Saito, T. Fukui, H. Takeda, H. Ohya, S. Kawata, Mucosal sulfhydryl compounds evaluation by in vivo electron spin resonance spectroscopy in mice with experimental colitis, Gut 52 (2003) 1291–1296.
[29] F. Tang, J.A. Hughes, Introduction of a disulfide bond into a cationic lipids enhances transgene expression of plasmid DNA, Biochem. Biophys. Res. Commun. 242 (1998) 141–145.
[30] F. Tang, J.A. Hughes, Use of dithioglycolic acid as a tether for cationic lipids increases the cytotoxicity and increases transgene expression of plasmid DNA in vitro, Bioconjug. Chem. 10 (1999) 791–796.
[31] V.V. Khramtsov, V.I. Yelinova, L.M. Weiner, T.A. Berezina, V.V. Martin, L.B. Volodarsky, Quantitative determination of –SH grups in low- and high-molecular-weight compounds by an electron spin resonance method, Anal. Biochem. 182 (1989) 58–63.
[32] V.V. Khramtsov, V.I. Yelinove, Yu.I. Glazachev, V.A. Rezmikov, G. Zimmer, Quantitative determination and reversible modification of thiols using imidazolidine biradical disulfide label, J. Biochem. Biophys. Meth. 35 (1997) 115–128.
[33] N.M. Kocherginsky, Y.Y. Kostetski, A.I. Smirnov, Use of nitroxide spin probes and electron paramagnetic resonance for assessing reducing power of beer. Role of SH groups, J. Agric. Food Chem. 53 (2005) 1052–1057.
[34] F. Vinello, F. Momo, M. Scarpa, A. Rigo, Kinetics of nitroxide spin label removal in biological systems: an in vitro and in vivo ESR study, Magn. Res. Imaging 13 (1995) 219–226.
[35] C. Mathieu, A. Mercier, D. Witt, L. Debmkowski, P. Tordo, b-Phosphorylated nitroxides in the pyrrolidine series: reduction by ascorbate, Free Radic. Biol. Med. 22 (1997) 803–806.
[36] N.M. Kocherginsky, N.I. S'yakste, M.A. Berkovich, V.M. Devychensky, Reduction of spin probes with ascorbic acid in solution and on biomembranes, Biofizika 26 (1981) 442–447.
[37] M. Schara, M. Nemec, S. Pecar, The involvement of uric acid un the scavenging of nitroxide radicals by ascorbate, Acta Chim. Slov. 47 (2000) 39–46.
[38] A.A. Bobko, I.A. Kirilyuk, I.A. Grigor'ev, J.L. Zweier, V.V. Khramtsov, Reversible reduction of nitroxides to hydroxylamines: role for ascorbate and glutathione, Free Radic. Biol. Med. 42 (2007) 404–412.